

# Multiscale Iris Representation for Person Identification

Vijay M. Mane  
Department of Electronics,  
Vishwakarma Institute of  
Technology, Pune, India.

Gaurav V. Chalkikar  
Department of Electronics,  
Vishwakarma Institute of  
Technology, Pune, India.

Milind E. Rane  
Department of Electronics,  
Vishwakarma Institute of  
Technology, Pune, India.

## ABSTRACT

Reliable automatic recognition of persons has long been an attractive goal. As in all pattern recognition problems, the key issue is the relation between interclass and intra-class variability: objects can be reliably classified only if the variability among different instances of a given class is less than the variability between different classes. In line with the requirement the proposed work of automated iris recognition is presented as a biometrics based technology for personal verification. The motivation for this endeavor stems from the observation that the human iris provides a particularly interesting structure on which to base a technology for noninvasive biometric assessment. A multiscale approach is used for Iris recognition and it is compared with Log-Gabor filter approach, the proposed one gives the satisfactory results.

## Keywords

Iris recognition, Multiscale representation, Laplacian of Gaussian (LOG), Log Gabor Filter, MSE.

## 1. INTRODUCTION

In today's information technology world, security for systems is becoming more and more important. The three main types of authentication are something you know (such as a password), something you have (such as a card or token), and something you are (biometric). Passwords are notorious for being weak and easily crackable due to human nature and our tendency to make passwords easy to remember or writing them down somewhere easily accessible. Cards and tokens can be presented by anyone and although the token or card is recognizable, there is no way of knowing if the person presenting the card is the actual owner. Biometrics, on the other hand, provides a secure method of authentication and identification, as they are difficult to replicate and steal. Biometric verification utilizes physiological and behavioral characteristics to verify a person's identity. Biometric recognition [1] systems verify a person's identity by analyzing his/her physical features or behavior (e.g. face [2], fingerprint[3], palmprint [4] iris[5], voice, signature, keystroke rhythms). In particular, the biomedical literature suggests that irises are as distinct as fingerprints or patterns of retinal blood vessels. Among many biometrics techniques, iris recognition is one of the most promising approaches due to its high reliability for personal identification [1–9]. Iris recognition is a method of biometric authentication that uses pattern recognition techniques based on high-resolution images of the irises of an individual's eyes. A major approach for iris recognition today is to generate feature vectors corresponding to individual iris images and to perform iris matching based on some distance metrics [5–7]. Most of the commercial iris recognition systems implement a famous algorithm using iris codes proposed by Daugman [5]. One of the difficult problems in feature-based iris recognition is that the matching performance is significantly influenced by many parameters in feature extraction process (e.g., spatial position,

orientation, center frequencies and size parameters for 2D Gabor filter kernel), which may vary depending on environmental factors of iris image acquisition. The human iris contains around 266 visible patterns, which forms the basis of several recognition algorithms [6]. The iris is unique to an individual and is stable with age [7]. This is a key advantage of iris recognition as its stability, or template longevity as, barring trauma, a single enrollment can last a lifetime. Wildes [10] started the segmentation of the iris ring by the construction of a binary edge-map. Next, used the circular Hough transform to fit circles that delimit the iris ring. This is the most usually seen method in the iris segmentation literature and is proposed with minor variants by [11–14]. The method proposed by Du et al. [15] is based on the previous detection of the pupil. The image is then transformed into polar coordinates and the iris outer border localized as the largest horizontal edge resultant from Sobel filtering. Morphologic operators were applied by Mira et al. [16] to find both iris borders. They detected the inner border by sequentially using threshold, image opening and closing techniques. The outer border was similarly detected. Eric Sung et al. proposed complexity measure based on maximum Shannon entropy of wavelet packet reconstruction to quantify the iris information [17]. Jiali Cui et al. proposed [18] the iris recognition algorithm based on PCA is first introduced. Lee et al. have introduced [19] the invariant binary feature which is defined as iris key. Kazuyuki et al. developed [20] phase-based image matching algorithm. Fusion of more than one biometrics makes the system more robust and accurate[21–22]. In this paper a biometric system based on multiscale approach for iris features is proposed for personal verification.

This paper has been organized in the following way. The iris recognition system is divided into three parts: image acquisition, iris localization and pattern matching. Image acquisition, iris localization are described in Section 2. In Section 3 the algorithm used for feature extraction and matching by calculating the mean square error is explained. Section 4 defines the Log-Gabor filter approach for iris recognition using Daugman's method. Section 5 states the comparative results of proposed method and Log-Gabor method. Section 6 gives the concluding remarks.

## 2. PROPOSED IRIS RECOGNITION SYSTEM

Block diagram of the proposed iris recognition system is as shown in Figure 1 that contains the typical stages of iris recognition system.

### 2.1 Image acquisition

The system captures eye images with the iris diameter typically between 100 and 200 pixels from a distance of 15–46 cm using a 330-mm lens.

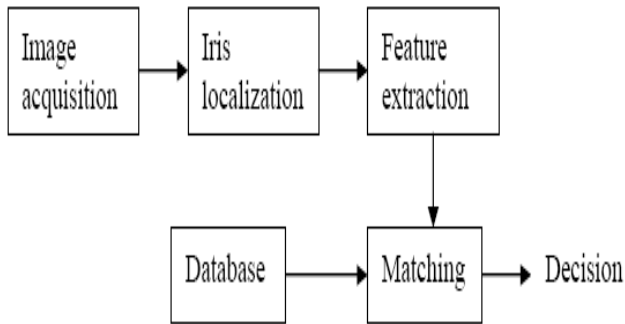


Fig 1: Proposed iris recognition system

## 2.2 Iris localization

Image acquisition of the iris cannot be expected to yield an image containing only the iris. It will also contain data derived from the surrounding eye region. Therefore, prior to iris pattern matching, it is important to localize that portion of the image derived from inside the limbs (the border between the sclera and the iris) and outside the pupil. If the eyelids are occluding part of the iris, then only that portion of the image without the eyelids should be included.

For the localization of iris first any random circular contour is formed which contains iris + pupil region to eliminate the remaining portion of the eye. A circular pseudo image is formed of desired diameter. The inside region of the circle is set at gray level '1'(white) and the outside region to '0'(black). The diameter selected is such that the circular contour will encircle the entire iris. This is done by detecting the radius and center points coordinates of iris using Hough transform. Thus when the product of the gray levels of the circular pseudo image and the original iris image are taken, the resultant image will have the circular contour enclosing the iris patterns and the outside of the circular contour will be at gray level '0'(black).

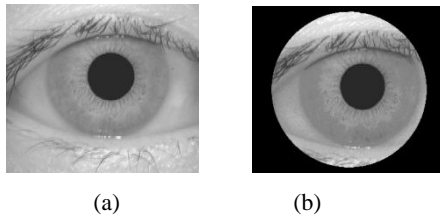


Fig 2. (a)eye image (b) circular contour around iris

The resultant image is the localized iris image. This circular contour is placed such that it is concentric with the pupil. So before pattern-matching, alignment is carried out. The iris and pupillary boundary of the iris are concentric about the pupillary center. So our aim is to determine the pupillary center. Firstly, we use point image processing techniques such as thresholding and gray-level slicing (without the background) on the resultant localized image to eliminate every other feature except the pupil of the eye. The pupil of the eye is set at gray level '0' and rest of the region is at '255'(white).

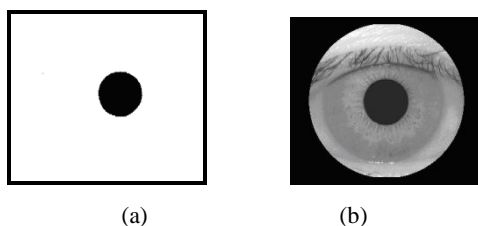


Fig 3. (a) Binary Pupil (b) Alignment of Iris

Next step involves determining the center of the pupil. This is done by finding the row and column having the maximum number of pixels of gray level '0' (black), which corresponds to the center of the pupil. Knowing the center of the pupil, we now shift the center of the circular contour to the center of the pupil. The resultant image will have the pupil and the iris regions concentric with the circular contour and the localized iris image to the center of frame is performed as shown in Figure 4.

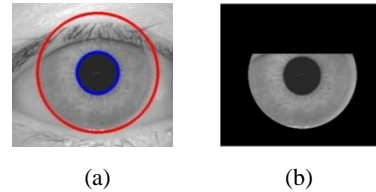


Fig 4. (a) Localized iris (b) Image removing eyelids

Final Result of iris localization eye with iris and pupil are circled correctly. Removing the portion of the iris occluded by the eyelids is carried out next. The eyelids are occluding part of the iris, so only that portion of the image below the upper eyelids and above the lower eyelids are included. This is achieved by changing the gray level above the upper eyelids and below the lower eyelids to '0'.

## 3. FEATURE EXTRACTION USING LAPLACIAN OF GAUSSIAN

The localized and aligned iris image is chosen that makes their distinctive patterns apparent. An isotropic, circularly symmetric band-pass decomposition derived from the application of Laplacian of Gaussian[23] filter to the image is obtained. This results in a pyramid formation of the iris image i.e. a Multiscale Representation which is used for iris pattern matching realized by the filter. The characteristics of the human iris are manifest at a variety of scales, distinguishing structures ranging from the overall shape of the iris. Multi-scale representation is used to capture the range of spatial detail to detect and characterize edges of the numerous iris patterns known. Multi-scale representation gives us iris images at varying spatial scales. These different structures give rise to edges at varying scales; small scales correspond to fine details and large scales correspond to gross structures. The images at each scale are obtained for classification of prominent edges of the different iris patterns at each level. Multi-scale representation is implemented using the pyramid algorithm of Laplacian of Gaussian (LOG) filters (4 levels) employing down sampling in the Gaussian and up sampling in the Laplacian of the Gaussian, filtered image. Besides being capable of making finer grained distinctions between different irises, this technique is of note for efficient storage and processing, as lower frequency bands are sub-sampled successively without loss of information beyond that introduced by the filtering.

The LoG filter can be specified as

$$\left(-\frac{1}{\pi\sigma^4}\right)\left(1 - \frac{\rho^2}{2\sigma^2}\right)e^{-\rho^2/2\sigma^2}$$

where  $\sigma$ —standard deviation of the Gaussian,  $\rho$ —radial distance of a point from the filter's center.

A discrete approximation which is derived from the above filter expression.

One dimensional mask  $w = \frac{[1 \ 4 \ 6 \ 4 \ 1]}{16}$ , two dimensional

mask  $W = w^T \times w$ ,

$w^T$ —transpose of the 1-D mask  $w$ . The resultant  $5 \times 5$  matrix mask

$$W = \frac{1}{16} \begin{bmatrix} 1 & 4 & 6 & 4 & 1 \\ 4 & 16 & 24 & 16 & 4 \\ 6 & 24 & 36 & 24 & 6 \\ 4 & 16 & 24 & 16 & 4 \\ 1 & 4 & 6 & 4 & 1 \end{bmatrix}$$

Now construction of the Laplacian Pyramid begins first with convolution of the Iris Image with LOG Mask 'W' so as to yield low-pass Gaussian filtered images  $g_k$

The expression is as follows:  $g_k = (W * g_{k-1})_{\downarrow 2}$

where  $k$  varies from 1 to 4,  $g_0$ —iris image of original scale,  $g_1$ – $g_4$ —low-pass Gaussian images each obtained after filtering the previous image and down sampling by 2,  $(\cdot)_{\downarrow 2}$  - down sampling by a factor of two in each image dimension.

Now after construction of low-pass Gaussian images at 4 different scales, the Laplacian pyramid  $l_k$  is formed as the difference between  $g_k$  and  $g_{k+1}$ , with  $g_{k+1}$  expanded before subtraction so that it matches the sampling rate of  $g_k$ . The expansion is accompanied by up sampling and interpolation:

$l_k = g_k - 4W * (g_{k+1})_{\uparrow 2}$  where  $(\cdot)_{\uparrow 2}$  indicates up sampling by a factor of 2.

Up sampling is achieved by the insertion of zeros between each row and column of the down sampled Gaussian image. The Mask 'W' is used as an interpolation filter and the factor 4 is necessary because 3/4 pixels are newly inserted zeros. The difference of Gaussians that this representation entails yields a good approximation to Laplacian of Gaussian filtering. The obtained Laplace of Gaussian images are as shown in Figure 5.

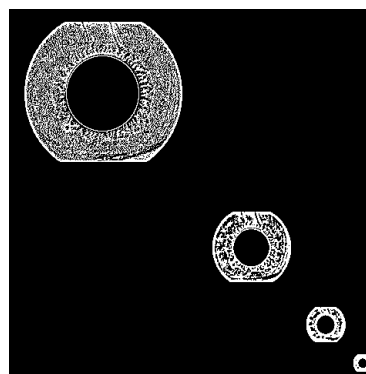


Fig 5. LOG representation of Iris image

We then evaluate the degree of match between the acquired image and images from the database. The approach taken is to quantify for the degree of match using mean square error between the acquired image and the images from the database as given below.

$$MSE = \frac{1}{n} \sum_{i=1}^x \sum_{j=1}^y (l_{-1}(i, j) - l_{-2}(i, j))^2$$

where  $(x, y)$  is size of image and  $n = x \times y$  is total number of pixels in image.

#### 4. FEATURE EXTRACTION USING LOG-GABOR FILTER

Once the iris region is successfully segmented from an eye image, the next stage is to transform the iris region so that it has fixed dimensions in order to allow comparisons. The normalization process will produce iris regions, which have the same constant dimensions. The homogenous rubber sheet model devised by Daugman [8] remaps each point within the iris region to a pair of polar coordinates  $(r, \theta)$  where  $r$  is on the interval  $[0, 1]$  and  $\theta$  is angle  $[0, 2\pi]$ .

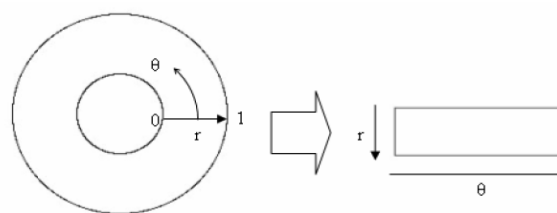


Fig 6. Daugman's Rubber Sheet Model.

For normalization of iris regions a technique based on Daugman's rubber sheet model was employed. The center of the pupil was considered as the reference point, and radial vectors pass through the iris region, as shown in Figure 6. A number of data points are selected along each radial line and this is defined as the radial resolution. The number of radial lines going around the iris region is defined as the angular resolution. Since the pupil can be non-concentric to the iris, a remapping formula is needed to rescale points depending on the angle around the circle. This is given by.

$$r' = \sqrt{\alpha\beta} \pm \sqrt{\alpha\beta^2 - \alpha - r_i^2}$$

with 
$$\alpha = O_x^2 + O_y^2$$
  
and 
$$\beta = \text{COS}(\pi - \arctan(\frac{O_x}{O_y}) - \theta)$$

where displacement of the center of the pupil relative to the center of the iris is given by  $O_x, O_y$ , and  $r$  is the distance between the edge of the pupil and edge of the iris at an angle,  $\theta$  around the region, and  $r$  is the radius of the iris as shown in Figure 7. The remapping formula first gives the radius of the iris region ‘doughnut’ as a function of the angle  $\theta$ .

A constant number of points are chosen along each radial line, so that a constant number of radial data points are taken, irrespective of how narrow or wide the radius is at a particular angle. From the ‘doughnut’ iris region, normalization produces a 2D array with horizontal dimensions of angular resolution and vertical dimensions of radial resolution. Another 2D array was created for marking reflections, eyelashes, and eyelids detected in the segmentation stage. In order to prevent non-iris region data from corrupting the normalized representation, data points which occur along the pupil border or the iris border are discarded.

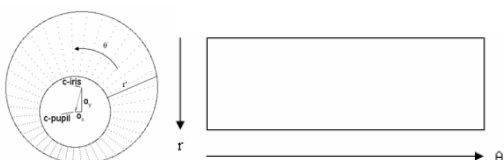


**Fig 7. Normalization with radial resolution of 20 pixels, and angular resolution of 240 pixels.**

The normalization process proved to be successful, a constant number of points are chosen along each radial line, here 20 pixel points are chosen as number of radial data points are taken, and 240 pixel points for angular data points are selected to create a 2D array, as shown in Figure 8.

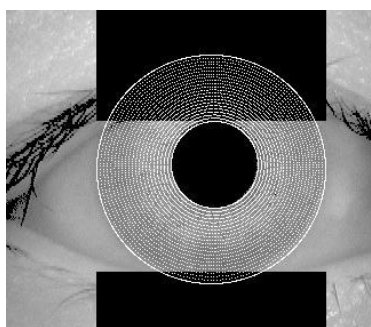


**Fig 8. Radial and angular pixel from iris region**

After iris region is segmented, to provide accurate recognition of individuals, the most discriminating information present in an iris pattern must be extracted to create a biometric template. Only the significant features of the iris must be encoded so that comparisons between templates can be made. Gabor filters are able to provide optimum conjoint representation of signal in space and spatial frequency. Normalization produces a 2D array with horizontal dimensions of angular resolution and vertical dimensions of radial resolution as shown in Figure 9.

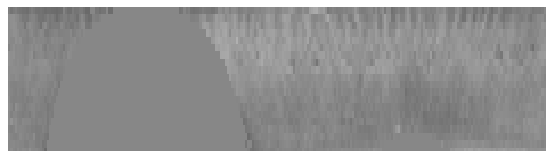


**Fig 9. Normalized Iris (Polar array)**

Another 2D array for marking reflections, eyelashes, and eyelids to prevent non-iris region data from corrupting the normalized representation, as shown in Figure 10 below.



**Fig 10. Mask for normalized iris (Polar Mask)**

A Log Gabor filter is used because Gabor filter have disadvantage that is the even symmetric filter will have a DC component whenever the bandwidth is larger than one octave. However, zero DC component can be obtained for any bandwidth by using a Gabor filter which is Gaussian on a logarithmic scale, this is known as the Log-Gabor filter. The frequency response of a Log-Gabor filter is given as;

$$G(f) = \exp\left(\frac{-(\log(f / f_o))^2}{2(\log(\sigma / f_o^2))}\right)$$

Where  $f_o$  represents the center frequency, and  $\sigma$  gives the bandwidth of the filter.

In comparing the bit patterns  $X$  and  $Y$ , the Hamming distance, HD, is defined as the sum of disagreeing bits (sum of the exclusive-OR between  $X$  and  $Y$ ) over  $N$ , the total number of bits in the bit pattern as given below.

$$HD = \frac{1}{N} \sum_{j=1}^N X_j (XOR) Y_j$$

The obtained HD's are normalized for comparison.

## 5. RESULT

The result obtained after experimentation are calculated. For experimentation the CASIA [24] database is used. The percentage Accuracy Based on FAR (False Acceptance Ratio), FRR (False Reject Ratio) and RAR (Right Acceptance Ratio) of the Proposed algorithm for various thresholds are given in Table 1 and Log-Gabor filter are given in Table 2

**Table 1. Result in terms of RAR, FRR, FAR for LOG**

Threshold	RAR	FRR	FAR
0.57	82.67	17.33	1.61
0.58	86	14	1.90
0.59	92	8	2.48
0.60	96	4	2.89
0.61	98	2	3.59
0.62	100	0	4.14

**Table 2. Result in terms of RAR, FRR, FAR for Log-Gabor**

Threshold	RAR	FRR	FAR
0.57	68	32	0.0408
0.58	86.66	13.33	0.040
0.59	92.66	7.33	0.0816
0.60	94.66	5.33	2.64
0.61	97.33	2.66	11.93
0.62	98.33	1.66	20.64

## 6. CONCLUSIONS

The developed system of Biometrics using multiscale representation and Log Gabor filter for person verification are tested and the results are all described earlier. The results of multiscale representation are better as compared to Log Gabor filter. The results of multiscale representation shows a good separation of intra-class and inter-class for different persons. If selected threshold is changed according to minimum square error such that if we select the maximum minimum square error of that particular Person, and considering same as threshold for decision it can improve decision making accuracy.

## 7. ACKNOWLEDGMENTS

Our thanks to the Dhananjay Theckedath for his cooperative help towards development of the work presented.

## 8. REFERENCES

- [1] Jain A.K., Ross A, Prabhakar S. 2004, "An introduction to biometric recognition," IEEE transactions on circuits and systems for video technology—special issue on image and video-based biometrics, vol. 14(1).
- [2] Satyajit Kautkar, Rahul Kumar Koche, Tushar Keskar, Aniket Pande, Milind Rane, Gary A. Atkinson 2010, "Face Recognition Based on Ridgelet Transforms," Procedia Computer Science 2 (ICEBT 2010), pp. 35–43.
- [3] Shekhar Suralkar, Milind E Rane, Pradeep M. Patil 2009, "Fingerprint Classification Based on Maximum Variation in Local Orientation Field," Proceedings of the 2009 IEEE International Conference on Systems, Man, and Cybernetics San Antonio, TX, USA, pp.945-948.
- [4] Priyanka Somvanshi, Milind E. Rane 2012, "Survey of Palmprint Recognition," International Journal of Scientific & Engineering Research, Vol.3, Issue2, pp.1-7.
- [5] Daugman J G 1998, "Recognizing people by their iris patterns," Information Security Technical Report, Vol. 3, Issue 1, pp.33-39.
- [6] Daugman J G 2003, "The importance of being random: statistical principles of iris recognition," Pattern Recognition, Vol. 36, Issue 2, pp.279-291.
- [7] Daugman J G 2005, "How Iris Recognition Works," Handbook of Image and Video Processing (2nd ed), pp. 1251-1262.
- [8] Kawaguchi, T, Rizon, M 2003, "Iris detection using intensity and edge information," Pattern Recognition, Vol. 36, Issue 2, pp. 549-562.
- [9] Bowyer, K W, Hollingsworth, K P, Flynn, P J 2008, "Image Understanding for Iris Biometrics: A survey," CVIU, pp. 281-307.
- [10] Wildes R. P. 1997, "Iris recognition: an emerging biometric technology," Proceedings IEEE, vol. 85(9), pp. 1348–1363.
- [11] L. Ma, T. Tan, Y. Wang, and D. Zhang 2003, "Personal Identification Based on Iris Texture Analysis," IEEE Transactions on Pattern Analysis and Machine Intelligence, 25(12), pp.1519-1533.
- [12] L.Ma, Y.Wang, D.Zhang 2004, "Efficient iris recognition by characterizing key local variations," IEEE Transactions on Image Processing, vol. 13, no. 6, pp. 739–750.
- [13] J. Huang, Y. Wang, T. Tan, and J. Cui 2004, "A new iris segmentation method for recognition," in Proceedings of the 17th International Conference on Pattern Recognition (ICPR04), vol. 3, pp. 23–26.
- [14] L. Ma, Y. Wang, and T. Tan 2002, "Iris recognition using circular symmetric filters," 25th International Conference on Pattern Recognition (ICPR02), vol. 2, pp. 414–417.
- [15] Y. Du, R. Ives, D. Etter, T. Welch, and C. Chang 2004, "A new approach to iris pattern recognition," in Proceedings of the SPIE European Symposium on Optics/Photonics in Defence and Security, vol. 5612, pp. 104–116.
- [16] J. Mira and J. Mayer 2003, "Image feature extraction for application of biometric identification of iris - a morphological approach," in Proceedings of the 16th Brazilian Symposium on Computer Graphics and Image Processing (SIBGRAPI 2003), Brazil, pp. 391–398.
- [17] E. Sung, X. Chen, J. Zhu and J. Yang 2002, "Towards non-cooperative iris recognition systems", Seventh international Conference on Control, Automation, Robotics And Vision (ICARCV'02), Singapore, pp. 990-995.
- [18] Jiali Cui, Y. Wang, J. Huang, T. Tan and Z. Sun 2004, "An Iris Image Synthesis Method Based on PCA and Super-resolution", IEEE 17th International Conference on Pattern Recognition (ICPR'04).
- [19] H. Gu Lee, S. Noh, K. Bae, K.-R. Park and J. Kim 2004, "Invariant biometric code extraction", IEEE Intelligent Signal Processing and Communication Systems, Proceedings IEEE ISPCS, pp. 181-184.
- [20] K Miyazawa, K Ito, T Aoki, K Kobayashi, H. Nakajima 2005, "An Efficient Iris Recognition Algorithm Using Phase-Based Image Matching", IEEE Image Processing Conference, 2005 (ICIP 2005), Vol. 2, pp. II- 49-52.
- [21] A. K. Jain and A. Ross 2004, "Multibiometric systems", Communications of the ACM, Vol. 47 (1), pp. 34-40.
- [22] Yogeshwari Borse, Rajnish Choubey, Roopali Soni, Milind E. Rane 2012, "Person Identification System Using Fusion of Matching Score of Iris," International Journal of Computer Science Issues – Vol. 9, Issue 3.
- [23] Balaji Ganeshan, Dhananjay Theckedath, Rupert Young, Chris Chatwin 2006, "Biometric iris recognition system using a fast and robust iris localization and alignment procedure," Optics and Lasers in Engineering, Vol. 44, pp.1–24.
- [24] Chinese Academy of Sciences. Specification of CASIA Iris Image Database (ver1.0). <http://www.nlpr.ia.ac.cn/english/irids/irisdatabase.htm>, March 2007.